Enhanced emission at 2.85 μm of Ho^{3+}/Pr^{3+} co-doped α-$NaYF_4$ single crystal*

WANG Cheng (王成)[1], **XIA Hai-ping** (夏海平)[1]**, **FENG Zhi-gang** (冯治刚)[1], **ZHANG Zhi-xiong** (张志雄)[1], **JIANG Dong-sheng** (江东升)[1], **ZHANG Jian** (张健)[1], **SHENG Qi-guo** (盛启国)[1], **TANG Qing-yang** (汤庆阳)[1], **HE Shi-nan** (何仕楠)[1], **JIANG Hao-chuan** (江浩川)[2], **and CHEN Bao-jiu** (陈宝玖)[3]

1. Key Laboratory of Photoelectronic Materials, Ningbo University, Ningbo 315211, China

2. Ningbo Institute of Materials Technology and Engineering, Chinese Academy of Sciences, Ningbo 315211, China

3. Department of Physics, Dalian Maritime University, Dalian 116026, China

(Received 5 November 2015)

The Ho^{3+}/Pr^{3+} co-doped $NaYF_4$ single crystals with various Pr^{3+} concentrations and constant Ho^{3+} molar percentage of ~1% were grown by an improved Bridgman method. Compared with the Ho^{3+} single-doped $NaYF_4$ crystal, an obviously enhanced emission band at 2.85 μm is observed under 640 nm excitation. The Judd-Ofelt strength parameters (Ω_2, Ω_4 and Ω_6) are calculated, the radiative transition probabilities (A), the fluorescence branching ratios (β) and the radiative lifetime (τ_{rad}) are obtained in the meantime. The energy transfer from Pr^{3+} to Ho^{3+} and the optimum fluorescence emission of Ho^{3+} ions around 2.85 μm are investigated. Moreover, the maximum emission cross section of above samples at 2.85 μm is calculated to be 0.72×10^{-20} cm^2 for the $NaYF_4$ single crystal with Ho^{3+} molar percentage of 1% and Pr^{3+} molar percentage of 0.5% according to the measured absorption spectrum. All results suggest that the Ho^{3+}/Pr^{3+} co-doped $NaYF_4$ single crystal may have potential applications in mid-infrared lasers.

Document code: A **Article ID:** 1673-1905(2016)01-0056-5

DOI 10.1007/s11801-016-5221-4

In the recent years, infrared solid state laser working around 3.0 μm have attracted much attention due to their extensive applications in telecommunications, remote sensing, military weapons, atmosphere transmission, optical parametric oscillators and broadband communication. Solid-state laser materials with rich rare earth ion-doped energy level structure has been investigated[1,2]. Ho^{3+} ion is one of the most important active ions applied to luminescence lasers because of its favorable energy level structure[3]. It has been demonstrated that infrared laser emission of Ho^{3+} ion acts in the range of 1.0—4.9 μm[4]. The $^5I_6\rightarrow{}^5I_7$ transition of Ho^{3+} ion can also emit a wide mid-infrared fluorescence in 2.85 μm.

The properties of Ho^{3+}/Pr^{3+} co-doped crystals have been investigated[5,6]. Due to the low phonon energy (<360 cm^{-1}), the wider optical transmittance and the high concentration doping trivalent rare earth ions which take the place of Y^{3+} ions, the $NaYF_4$ single crystal is favorable to be used as solid material for the mid-infrared laser[7]. As host matrix of laser materials, the $NaYF_4$ single crystal has excellent comprehensive properties[8]. However, Ho^{3+}/Pr^{3+} co-doped $NaYF_4$ crystal has not been successfully obtained due to the difficulties of crystal growth[9], and the optical properties of Ho^{3+}/Pr^{3+} co-doped $NaYF_4$ crystal focusing on 2.85 μm have never been reported.

In this paper, Ho^{3+}/Pr^{3+} co-doped $NaYF_4$ crystals were grown by the Bridgman method. The absorption and emission spectra were measured, the spectroscopic investigations of 2.85 mm emission were analyzed, and the optical gain properties were carried out. By analyzing these fluorescence characteristics, the mechanisms of 2.85 μm emission in Ho^{3+}/Pr^{3+} co-doped $NaYF_4$ crystal and the energy transfer processes between Pr^{3+} and Ho^{3+} are understood.

Ho^{3+} singly doped and Ho^{3+}/Pr^{3+} co-doped $NaYF_4$ crystals were grown by Bridgman method using KF as flux. The molar compositions of the raw materials were NaF: KF: YF_3: HoF_3: PrF_3=30: 18: 50.5: 1: x (x=0, 0.2, 0.5, 1). The detailed processes for crystal growth were described in Ref.[10]. The grown crystal with about Φ10 mm×77 mm were cut into pieces and polished to 2.2 mm-thick for the optical property measurements. The X-ray diffraction (XRD) patterns of samples were recorded with an XD-98X diffractometer (XD-3, Beijing). The absorption spectrum was detected by a Cary 5000 UV/VIS/NIR spectrophotometer in the wavelength region from 200 nm to 2 500 nm. The emission spectra

* This work has been supported by the National Natural Science Foundation of China (No.51272109), the Natural Science Foundation of Ningbo City (No.201401A6105016), and the K. C. Wong Magna Fund in Ningbo University.

** E-mail: hpxcm@nbu.edu.cn

were tested by a Traix 320 type spectrometer (Jobin-Yvon Co., France) in the range of 1 000—1 800 nm and 1 800—3 020 nm excited by 640 nm light. All measurements were carried out at room temperature.

The XRD pattern of $NaYF_4$ single crystal doping with Ho^{3+}/ Pr^{3+} is shown in Fig.1(a), in which the peak positions are consistent with those in JCPD 77-2042 of $NaYF_4$[11] which is also listed in Fig.1(b). The similar XRD patterns demonstrate that all the crystals have been almost crystallized into pure tetragonal phase, and neither obvious peak shift nor second phase is caused in current doping level. The calculated cell parameters from the XRD pattern for this crystal are $a=b=c=0.550\ 2$ nm.

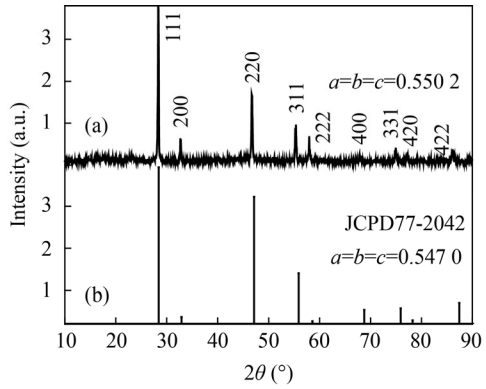

Fig.1 (a) Powder XRD pattern of Ho^{3+}/Pr^{3+} co-doped $LiYF_4$ crystal; (b) The standard line pattern of $NaFY_4$ (JCPDS 77-2042)

Fig.2 shows the absorption spectra of Ho^{3+}/Pr^{3+} co-doped α-NaYF4 crystals in the wavelength range from 300 nm to 2 200 nm. There are eight absorption bands at 360 nm, 416 nm, 449 nm, 483 nm, 536 nm, 640 nm, 1 158 nm and 1 936 nm, which are closely related to Ho^{3+} transitions from the ground state $^5I_8$ to $^3H_6$, $^5G_5$, $^5F_1$-$^5G_6$, $^5F_3$, $^5F_4$-$^5S_2$, $^5F_5$, $^5I_6$ and $^5I_7$ excited states, respectively. There is a strong absorption peak concentrated at 640 nm, which means that Ho^{3+} ion can act as an excellent activator to absorb the 640 nm pump light. The inset of Fig.2 shows the ground state absorption cross section around 640 nm. The full width at half the maximum (*FWHM*) of this band is about 25 nm, and the peak value of absorption cross section is 5.2×10^{-21} cm^2. Three new bands appear at 1 529 nm, 1 442 nm and 588 nm in the Ho^{3+}/Pr^{3+} co-doped $NaYF_4$ crystal besides eight absorption bands of Ho^{3+}. They are corresponding to the transitions from the ground state $^3H_4$ to $^3F_3$, $^3F_4$ and $^1D_2$ levels of Pr^{3+} ion, respectively.

The Judd-Ofelt (J-O) theory is extensively employed by determining the radiative properties of rare-earth ions within a matrix based on its absorption spectrum. According to the J-O theory[12,13], the J-O intensity parameters of Ω_2, Ω_4 and Ω_6 for the sample are calculated respectively from the absorption spectrum. The obtained J-O parameters of Ho^{3+} ions in Ho^{3+}/Pr^{3+} co-doped $NaYF_4$ and other crystals are presented in Tab.1. The obtained root mean square deviation δ_{rms} is as low as 0.62×10^{-6}, indicating the validity and reliability of the results[14].

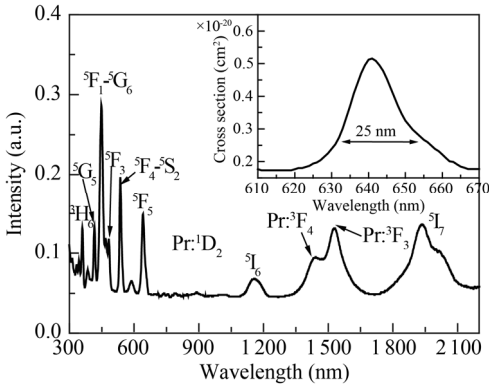

Fig.2 The absorption spectrum of Ho^{3+}/Pr^{3+} co-doped NaYF4 crystal with Ho:Pr=1:0.5 (The inset is the ground state absorption cross section around 640 nm.)

Tab.1 Comparison of J-O parameters of Ho^{3+} ions in Ho^{3+}/Pr^{3+} co-doped $NaYF_4$ and other crystals

Crystals	Ω_2	Ω_4	Ω_6
YAG:Ho^{3+}[15]	0.04	2.67	1.89
$LiLuF_4$: Ho^{3+}[16]	2.24	2.31	1.44
$NaYF_4$: Ho^{3+}[17]	1.65	0.84	1.61
$LiYF_4$: Ho^{3+}/Pr^{3+}[5]	1.52	1.96	1.05
$NaYF_4$: Ho^{3+}/Pr^{3+}	1.27	2.40	1.23

According to comparing with J-O parameters in Tab.1, it can be obtained that the value of Ω_2 in this paper is lower than those in other crystals. The value of Ω_2 is much lower, then the electrovalent bond is stronger, and the symmetry of crystal structure is much higher. This comparison confirms that the symmetry of α-$NaYF_4$ crystal structure is much stronger. The value of Ω_4/Ω_6 determines the spectroscopy quality of the host matrix. The Ω_4/Ω_6 of Ho^{3+}/Pr^{3+}:$NaYF_4$ single crystal is larger than that of other crystals, indicating the promising use in laser output[18].

The radiative rate A, the fluorescence branching ratios β and the radiative lifetime τ_{rad} are calculated as shown in Tab.2.

Tab.2 Calculated A, β and τ_{rad} of Ho^{3+} in Ho^{3+}/Pr^{3+}: α-$NaYF_4$ crystal

J	$\rightarrow J'$	λ (nm)	A (S^{-1})	β	τ_{rad} (ms)
$^5I_7$	$\rightarrow$ $^5I_8$	1 954	50.98	1.00	19.615 677
$^5I_6$	$\rightarrow$ $^5I_8$	1 160	102.09	0.89	8.730 572 0
	$\rightarrow$ $^5I_7$	2 858	12.45	0.11	

The mid-infrared emission spectra of Ho^{3+}/Pr^{3+} co-doped α~NaYF4 crystals with different Pr^{3+} concentrations and constant Ho^{3+} molar percentage of 1% are shown in Fig.3. A broad emission band centered at 2.85 μm owing to Ho^{3+}: $^5I_6$-$^5I_7$ transition can be observed in Fig.3. It can be seen from Fig.3 that the fluorescence intensity around 2.85 μm continues to rise as the doped Pr^{3+} molar percentage increases from 0% to 0.5%, however, the emission intensity drops when the doping level is further improved to 1%, because the higher doping concentration may lead to concentration quenching resulting in lower emission. In this work, the optimal mid-infrared emission intensity at ~2.85 μm is the sample with the doping concentrations of 1% Ho^{3+} and 0.5% Pr^{3+}.

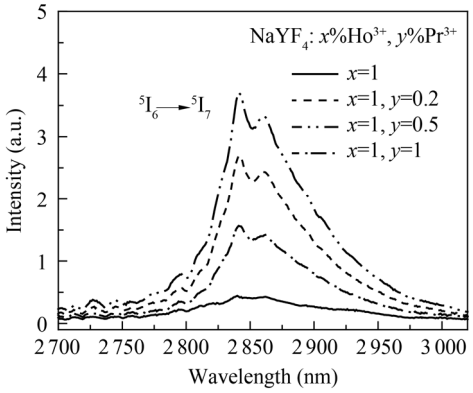

Fig.3 The Emission spectra at 2.85 μm of Ho^{3+}/Pr^{3+} co-doped $NaYF_4$ crystals with various doping concentrations

On the basis of the emission spectra of Ho^{3+}/Pr^{3+} co-doped α-$NaYF_4$ crystal, we further investigate the energy transfer of Pr^{3+} and Ho^{3+} in α-NaYF4 crystals. As we can see from Fig.4, the emission bands are located at 1.2 μm, 2.0 μm and 2.4 μm, which corresponds to the energy transfer of Ho^{3+}: $^5I_6 \rightarrow {}^5I_8$, Ho^{3+}: $^5I_7 \rightarrow {}^5I_8$ and Pr^{3+}: $^3H_6 \rightarrow {}^3H_4$, respectively. The introduction of Pr^{3+} ions with appropriate concentration can increase the fluorescence intensity of Pr^{3+} at 2.4 μm and make the fluorescence peak of Ho^{3+} at 2.0 μm with a very low luminous intensity.

In order to illuminate the mid-infrared fluorescence behavior, the energy transfer mechanism between Ho^{3+} and Pr^{3+} is analyzed, and the simplified energy level diagram between them is presented in Fig.5. When the sample is excited by 640 nm wavelength laser, the Ho^{3+} ions in ground state ($^5I_8$) is pumped to the $^5F_5$ state ($^5I_8$ + a photon$\rightarrow {}^5F_5$). It is obvious that ions in $^5I_6$ level can relax radiatively to the ground state and 1.2 μm emission happens ($^5I_6 \rightarrow {}^5I_8$ + 1.2 μm). Besides, a significantly low emission intensity of the $^5I_7$ level at 2.0 μm is observed in the Ho^{3+} and Pr^{3+} co-doped sample, which justifies that Pr^{3+} ions can be used effectively to depopulate the Ho^{3+}:$^5I_7$ level. On account of the energy levels of $^3F_2$ of Pr^{3+} and $^5I_7$ of Ho^{3+} match very well as shown in Fig.5, the energy transfer (Ho^{3+}:$^5I_7$, Pr^{3+}:$^3H_4$) → (Ho^{3+}:$^5I_8$, Pr^{3+}:$^3F_2$) can take place. The ions in Pr^{3+}:$^3F_2$ level nonradiatively decay to the lower Pr^{3+}:$^3H_6$ level, then radiatively decay to the Pr^{3+}:$^3H_4$ level, and emit a broadband emission around 2.4 μm as observed in Fig.4. It further demonstrates the existence of the energy transfer process from Ho^{3+} to Pr^{3+}.

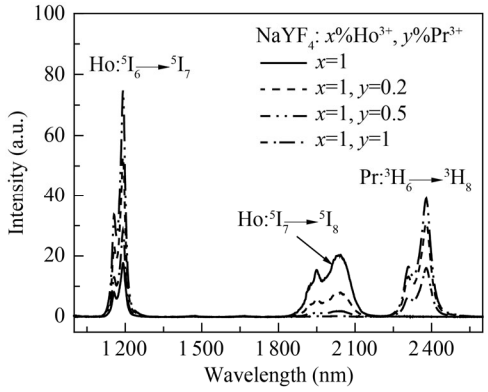

Fig.4 The Emission spectra at 1.2 μm, 2.0 μm and 2.4 μm of Ho^{3+}/Pr^{3+} co-doped $NaYF_4$ crystals with various doping concentrations

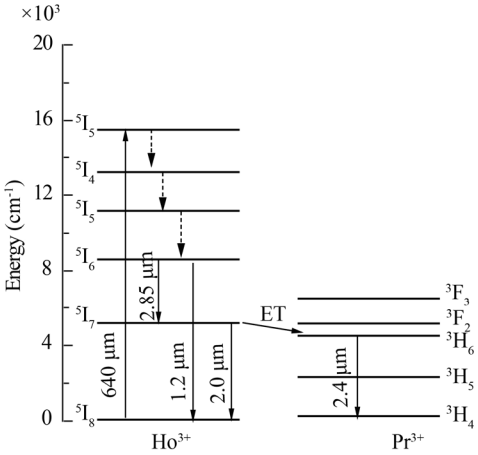

Fig.5 The energy level and simplified energy transfer diagram for Ho^{3+}/Pr^{3+}:$NaYF_4$ crystal pumped by 640 nm laser

However, 2.85 μm fluorescence is much more efficient in Ho^{3+}/Pr^{3+} co-doped α-$NaYF_4$ crystal with the introduction of Pr^{3+} ions. Part of Ho^{3+} ions in $^5I_6$ level may relax to the next lower $^5I_7$ level by radiative transition process, and this process generates 2.85 μm fluorescence ($^5I_6 \rightarrow {}^5I_7$ + 2.85 μm). It has been revealed that the Pr^{3+} ions can efficiently deactivate the first excited state ($^5I_7$) of Ho^{3+}, and the optimal Pr^{3+} concentration can be found to be 0.5%, which is in agreement with that of 2.85 μm emission. It is indicated that the Ho^{3+}/Pr^{3+} co-doped $NaYF_4$ crystal can successfully achieve the 2.85 μm emission and may be a potential media for 2.85 mm mid-infrared laser.

As an important spectroscopic parameter for laser

performance[19], the absorption and emission cross sections are calculated. According to the measured absorption spectra, the absorption cross section (σ_{abs}) can be determined as

$$\sigma_{abs}(\lambda) = 2.303\log(I_0 / I)/NL, \quad (1)$$

where L is the thickness of the polished crystal (L=2.2 mm in this paper), $\log(I_0/I)$ is the measured optical density taken from the measured absorption spectra, and N is the number of Ho^{3+} ions in per unit volume (cm^{-3}).

The stimulated emission cross section (σ_{em}) of $^5I_6 \rightarrow {}^5I_7$ transition can be calculated by McCumber theory as

$$\sigma_{em}(\lambda) = \sigma_{abs}(\lambda)\exp[\varepsilon - hc\lambda^{-1}/kT], \quad (2)$$

where k is the Boltzmann constant, T is temperature (here is the room temperature), λ is the transition wavelength, h is Planck constant, and ε is the zero-line energy defined as the energy gap between $^5I_6$ and $^5I_7$ manifolds at the constant temperature, and here ε=3 517 cm^{-1}[20].

The calculated absorption and emission cross sections of the $^5I_6 \rightarrow {}^5I_7$ transition by Eqs.(1) and (2) are shown in Fig.6. Obviously, the maximum emission cross section is higher than the maximum absorption cross section, and the maximum emission cross section of Ho^{3+}/Pr^{3+} co-doped $NaYF_4$ single crystal reaches 0.72×10^{-20} cm^2 (2.85 μm), which is higher than that of 0.68×10^{-20} cm^2 (2.9 μm) in Ho^{3+}/Pr^{3+} co-doped $LiYF_4$ crystal[7].

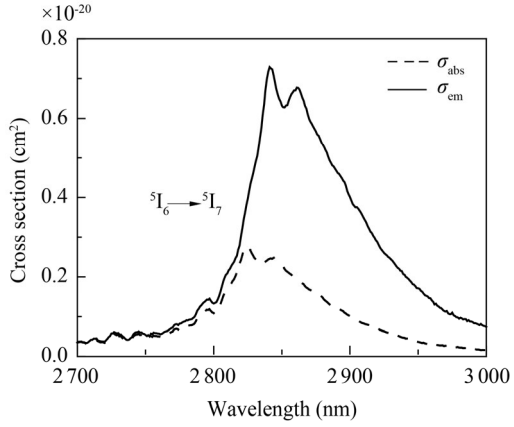

Fig.6 Absorption and emission cross sections for the transition Ho^{3+}:$^5I_6 \rightarrow {}^5I_7$ in Ho^{3+}/Pr^{3+}co-doped α-$NaYF_4$ crystal

Based on the calculated absorption and emission cross sections, the optical gain coefficient $g(\lambda)$ can be defined as

$$g(\lambda)=N_2\sigma_{em}-N_1\sigma_{abs}, \quad (3)$$

where N_2 and N_1 represent the population inversion volume-densities of the upper and lower levels, respectively. The total population inversion volume-density is $N=N_2+N_1$, and therefore the gain cross section spectrum $G(\lambda)$ is expressed as

$$G(\lambda)=P\sigma_{em}-(1-P)\sigma_{abs}. \quad (4)$$

The calculated gain cross sections for $^5I_6 \rightarrow {}^5I_7$ transition of Ho^{3+} as a function of wavelength with different P values are shown in Fig.7. From Eq.(3), it can be concluded that a larger gain cross section can be obtained when the emission one is bigger. As the value of P increasing from 0 to 1 with a step of 0.1, the positive gain appears at 2.85 μm when P is around 0.3. Evidently, it notes that the pump threshold to obtain the ~2.85 μm laser is likely to be lower, and it is beneficial to the infrared lasers.

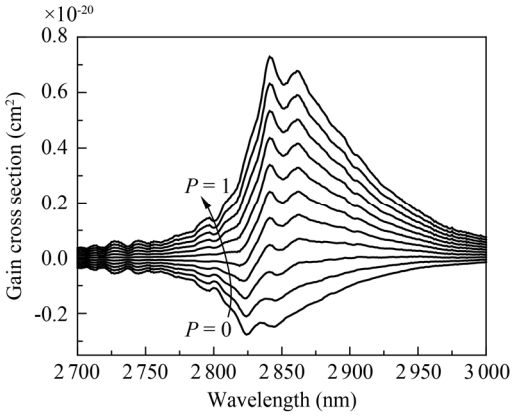

Fig.7 Gain cross section spectra of $^5I_6 \rightarrow {}^5I_7$ transition in Ho^{3+}/Pr^{3+} co-doped α-$NaYF_4$ crystal with P increasing from 0 to 1 with a step of 0.1

Ho^{3+}/Pr^{3+} co-doped α-$NaYF_4$ single crystals were grown successfully by the improved Bridgman method with KF as the flux which reduces the melting point of $NaYF_4$ and changes the phase equilibrium. The fluorescent emission at 2.85 μm, corresponding to $^5I_6 \rightarrow {}^5I_7$ transition, is observed under 640 nm excitation. The calculated maximum emission cross section at 2.85 μm ($^5I_6 \rightarrow {}^5I_7$) in Ho^{3+}/Pr^{3+} co-doped $NaYF_4$ crystal is 0.72×10^{-20} cm^2, which is larger than that of 0.68×10^{-20} cm^2 in $LiYF_4$ crystal. All these spectral properties show that the Ho^{3+}/Pr^{3+} co-doped $NaYF_4$ crystal may be a potential single crystal for 2.85 μm mid-infrared laser application.

References

[1] DONG Yan-ming, XIA Hai-ping, FU Li, LI Shan-shan, GU Xue-mei, ZHANG Jian-li, WANG Dong-jie, ZHANG Yue-pin, JIANG Hao-chuan and CHEN Bao-jiu, Optoelectronics Letters **10**, 262 (2014).

[2] GU Chang-Jiang, CHEN Xiang-ying, SUN Dun-lu, LUO Jian-qiao, CHEN Jia-kang, ZHANG Hui-li, ZHANG Qing-li and YIN Shao-tang, Journal of Optoelectronics·Laser **25**, 491 (2014). (in Chinese)

[3] Schweizer T., Samson B. N., Hector J. R., Brocklesby W. S., Hewak D. W. and Payne D. N., Infrared Physics & Technology **40**, 329 (1999).

[4] D. Lande, S. S. Orlov, A. Akella, L. Hesselink and R. R.

Neurgaonkar, Optics Letters **22**, 1722 (1997).
[5] Jiangtao Peng, Haiping Xia, Peiyuan Wang, Haoyang Hu, Lei Tang, Yuepin Zhang, Haochuan Jiang and Baojiu Chen, Journal of Materials Science & Technology **239**, 910 (2014).
[6] Rao B. V. and Buddhudu S., Journal of Materials Science **43**, 233 (2008).
[7] H. H. Yu, V. Petrov, U. Griebner, D. Parisi, S. Veronesi and M. Toneli, Optics Letters **37**, 2544 (2012).
[8] J. Hölsä, T. Laihinen, T. L. Laamanen, M. Lastusaari, L. Pihlgrn, L. C. V. Rodrigues and T. Soukka, Physica B: Condensed Matter **439**, 22 (2014).
[9] R. E. Thoma, G. M. Hebert, H. Insley and C. F. Weaver, Inorganic Chemistry **2**, 1005 (1963).
[10] H. B. Chen, S. J. Fan, H. P. Xia and J. Y. Xu, Journal of Materials Science Letters **21**, 457 (2002).
[11] M. Misiak, K. Prorok, B. Cichy, A. Bednarkiewicz and W. Strek, Optical Materials **35**, 1124(2013).
[12] B. R. Judd,. Physical Review **127**, 750 (1962).
[13] G. S. Ofelt, Journal of Chemical Physics **37**, 511 (1962).
[14] Cai M., Wei T., Zhou B., Tian Y., Zhou J., Xu S. and Zhang J., Journal of Alloys & Compounds **626**, 165 (2015).
[15] M. Malinowski, Z. Frukacz, M. Szufinsk, A. Wnuk and M. Kaczkan, Journal of Alloys & Compounds **300-301**, 389 (2000).
[16] C. C. Zhao, Y. Hang, L. H. Zhang, J. G. Yin, P. C. Hu and E. Ma, Optical Materials **33**, 1610 (2011).
[17] Yang S., Xia H., Zhang J., Jiang Y., Shi Y., Gu X., Zhang J., Zhang Y., Jiang H. and Chen B., Optical Materials **45**, 209 (2015).
[18] Di J., Xu X., Xia C., Sai Q., Zhou D., Lv Z. and Xu J., Journal of Luminescence **155**, 101 (2014).
[19] B. Peng and T. Izumitani, Optical Materials **4**, 797 (1995).
[20] B. M. Walsh, N. P. Barnes and B. D. Bartolo, Journal of Applied Physics **83**, 2772 (1998).